

transport site. Work in another laboratory (P. Low, personal communication) has shown that the B<sub>2</sub> and C transitions can be reconstituted into model systems by using appropriate fragments of band 3 obtained by mild proteolysis and chromatographic separation.

The TGA method is, therefore, capable of providing detailed information on the participation of erythrocyte proteins in various cooperative structural changes occurring in the membrane. The method depends on thermal cross-linking through the formation of intermolecular disulfide bonds, which are in all likelihood triggered by the reorganization of membrane components and/or the unfolding of certain proteins. The method appears to have general applicability, and preliminary results on other membrane systems are encouraging.

## References

- Bennett, V., & Stenbuck, P. J. (1979a) *Nature (London)* **280**, 468-473.
- Bennett, V., & Stenbuck, P. J. (1979b) *J. Biol. Chem.* **254**, 2533-2541.
- Brandts, J. F., Erickson, L., Lysko, K. A., Schwartz, A. T., & Taverna, R. D. (1977) *Biochemistry* **16**, 3450-3454.
- Brandts, J. F., Taverna, R. D., Sadasivan E., & Lysko, K. A. (1978) *Biochim. Biophys. Acta* **512**, 566-578.
- Jackson, W. M., & Brandts, J. F. (1970) *Biochemistry* **9**, 2294-2301.
- Jackson, W. M., Kostyla, J., Nordin, J. H., & Brandts, J. F. (1973) *Biochemistry* **12**, 3662-3667.
- Jenkins, R. E., & Tanner, M. J. (1977) *Biochem. J.* **161**, 131-138.
- Kahlenberg, A. (1976) *J. Biol. Chem.* **251**, 1582-1590.
- Luna, E. J., Kidd, G. H., & Branton, D. (1979) *J. Biol. Chem.* **254**, 2526-2532.
- Lux, S. E. (1979) *Sem. Hematol.* **16**, 24.
- Rothstein, A., Knaut, P., Grinstein, S., & Shami, Y. (1979) in *Normal and Abnormal Red Cell Membranes* (Ed.'s: Lux, S., Marchesi, V., & Fox, C. F., Eds.) pp 483-496, Liss, New York.
- Sheetz, M. P. (1979) *Biochim. Biophys. Acta* **557**, 122-134.
- Snow, J., Brandts, J. F., & Low, P. (1978) *Biochim. Biophys. Acta* **512**, 579-591.
- Snow, J., Vicentelli, J., & Brandts, J. F. (1981) *Biochim. Biophys. Acta* **642**, 418-428.
- Steck, T. (1978) *J. Supramol. Struct.* **8**, 311-324.
- Steck, T., & Yu, J. (1973) *J. Supramol. Struct.* **1**, 220-232.
- Strapazon, E., & Steck, T. L. (1977) *Biochemistry* **16**, 2966-2970.
- Tyler, J. M., Hargreaves, W. R., & Brandon, D. (1979) *Proc. Natl. Acad. Sci. U.S.A.* **76**, 5192-5196.
- Yu, J., & Steck, T. L. (1975) *J. Biol. Chem.* **250**, 9176-9184.
- Zacharius, R., Zell, T., Morrison, J., & Woodlock, J. (1969) *Anal. Biochem.* **30**, 148-152.

## Comparative Study of an Adenosine Triphosphatase Trigger-Fused Lipid Vesicle and Other Vesicle Forms of Dimyristoylphosphatidylcholine<sup>†</sup>

Jean-Pierre Dufour, Ray Nunnally,<sup>‡</sup> Loren Buhle, Jr., and Tian Yow Tsong\*

**ABSTRACT:** Several known forms of bilayer vesicles of dimyristoylphosphatidylcholine exhibit the gel to liquid-crystalline phase transition in the temperature range convenient for membrane enzyme reconstitution studies. This warrants a systematic investigation of their physical characteristics and their phase transition behaviors. We have employed electron microscopy, gel chromatography, <sup>31</sup>P nuclear magnetic resonance, differential scanning microcalorimetry, and fluorescence spectroscopy to determine several physical parameters of the limiting size microvesicle (260 ± 40 Å), the larger vesicle form (900 ± 100 Å) of Enoch and Strittmatter [Enoch, H. G., & Strittmatter, P. (1979) *Proc. Natl. Acad. Sci. U.S.A.* **76**, 145], the multilamellar vesicle, and, in particular, an ATPase-trigger-fused macrovesicle (950 ± 200 Å). This latter vesicle form was produced by a spontaneous fusion of the complex of the plasma membrane ATPase of *Schizosaccharomyces pombe*

and the lipid microvesicles at a low ratio of enzyme to vesicle concentrations, and at a low temperature (around 10 °C). The ATPase-trigger-fused vesicles are unilamellar and have an intact ionic permeation barrier at 30 °C and a gel to liquid-crystalline transition temperature at 24.4 °C with a transition heat of 5.64 kcal/mol. Thus, this vesicle form should be a valuable tool for studying possible proton-pumping activity of this ATPase. In contrast to data found in the literature, which show lack of the pretransition for unilamellar microvesicles, we have observed the pretransition around 15 °C for all the vesicle forms examined. Moreover, the transition widths of unilamellar vesicles are much broader than those of the multilamellar vesicles, suggesting that in the latter system interlayer interactions may contribute to the cooperativity of the transition.

**A**tttempts have been made to prepare lipid vesicle systems that possess desired properties for membrane enzyme re-

stitution studies. The relevant features of the vesicle systems include, for example, an easy and complete incorporation of proteins, an intact and well-defined ionic permeation barrier, and, most importantly, the retention or the reactivation of the biological activity of proteins. Another useful feature of the lipid vesicles is the phase transition property, which would allow studies of the effect of lipid conformational states on the biological activity of enzymes. Dimyristoyl-

<sup>†</sup> From the Department of Physiological Chemistry, The Johns Hopkins University School of Medicine, Baltimore, Maryland 21205. Received January 21, 1981. This work was supported by National Institutes of Health Grant GM28795.

<sup>‡</sup> Present address: Department of Radiology, University of Texas Health Science Center, Dallas, TX 75235.

phosphatidylcholine (DMPC)<sup>1</sup> exhibits a gel to liquid-crystalline transition temperature, convenient for membrane enzyme reconstitution studies. However, most physical characterizations of DMPC dispersions in water have been performed with multilamellar vesicle systems, and only limited data are available for the unilamellar microvesicles and other forms of lipid structures [for reviews, see Mabrey & Sturtevant (1979), Bergelson (1978), and O'Neill & Richards (1980)].

We have been studying the plasma membrane ATPase of the yeast *Schizosaccharomyces pombe* in connection with its function as a proton pump. This enzyme is the only ATPase of its class that has been fully characterized in its purified form (Dufour & Goffeau, 1978, 1980a,b; Dufour et al., 1980). It has a single-type peptide chain of 100 000 daltons which forms a phosphorylated intermediate (Amory et al., 1980). Although indications suggesting its proton-pumping activity have been obtained from in vivo studies (Foury & Goffeau, 1975; Foury et al., 1977; Serrano, 1980), full demonstration must await its reconstitution into a well-characterized lipid vesicle system where other unknown sources of membrane activity can be eliminated.

In our attempt to incorporate this ATPase into different forms of DMPC vesicles, we have observed that the purified plasma membrane ATPase induced a significant increase of the turbidity of DMPC microvesicles below the phospholipid phase transition, suggesting the formation of a larger structure (Dufour & Tsong, 1981). Light-scattering data do not permit us to determine if the large structures resulted from simple vesicle aggregation or from fusions of vesicles.

In this work, these enzyme-trigger-fused structures (to be called p-UMV) have been characterized together with other known forms of lipid vesicles, microvesicles, macrovesicles [by the method of Enoch & Strittmatter (1979)], and multilamellar vesicles. Although synthetic lecithins are widely used, DMPC vesicles are still poorly characterized regarding <sup>31</sup>P NMR and DSC analyses [for reviews, see Mabrey & Sturtevant (1979), Bergelson (1978), and O'Neill & Richards (1980)]. It is demonstrated that the p-UMV are unilamellar macrovesicles which can be useful for the functional study of this enzyme. Moreover, as DMPC microvesicles and macrovesicles have characteristic phase transition temperatures in a range where many enzymes are active, they can be used to demonstrate lipid-enzyme interactions in Arrhenius studies.

## Materials and Methods

**Chemicals.** ATP (disodium salt, grade II), egg lysolecithin, bovine serum albumin, and deoxycholic acid were obtained from Sigma. DMPC and DPPC were purchased from Calbiochem. ANS was obtained from Baker Chemical. Sephadex G-25, Sepharose 4B, Sepharose CL-2B and Blue dextran 200 were purchased from Pharmacia Fine Chemicals. [*carboxyl*-<sup>14</sup>C]Deoxycholic acid and [<sup>14</sup>C]sucrose were from ICN Pharmaceuticals. Other reagents were of the purest commercially available grade. The plasma membrane ATPase of the yeast *S. pombe* has been purified as described by Dufour

& Goffeau (1978). <sup>35</sup>S-Labeled plasma membranes of *S. pombe* were the generous gift of Dr. A. Goffeau (Catholic University of Louvain-la-Neuve, Belgium).

**Preparation of Phospholipid Dispersions.** The DMPC purchased from Calbiochem (lot no. 429475) exhibited a transition width of 0.085 °C by differential scanning calorimetry (see Results) and was used without further purification. Four types of DMPC dispersions were prepared. The first one corresponds to the *multilayered vesicles* of Bangham et al. (1974). DMPC was dispersed at 15 mg/mL in 10 mM Tris and 20 μM EDTA, adjusted to pH 7.5 with acetic acid, at 30 °C by vortexing the sample. The suspension was then incubated at 30 °C for 1 h and kept thereafter in the refrigerator for no more than 1 day. The second type of DMPC dispersion corresponds to the *unilamellar microvesicles* described by Huang (1969). DMPC was suspended at 2 mg/mL in the sonication buffer containing 10 mM Tris and 20 μM EDTA adjusted to pH 7.5 with acetic acid. This suspension was placed in a water-jacketed glass tube and sonicated by using a Biosonik IV sonicator (VWR Scientific) with a standard titanium probe at 60-W power level for 30 min (15 s on, 15 s off) at 31 °C. This alternate sonication prevented sample solutions from overheating. After the sonication, the lipid dispersion was centrifuged at 100 000g in a Beckman R65 rotor at 24 °C for 1 h. Two-thirds of the upper part of the supernatant was removed and kept at room temperature. The microvesicles were used immediately. The third type corresponds to the *unilamellar macrovesicles* (d-UMV) described by Enoch & Strittmatter (1979). DMPC was suspended at 20 mg/mL in 10 mM Tris, 20 μM EDTA, 1 mM NaN<sub>3</sub>, and 0.1 M NaCl, adjusted to pH 7.5 with acetic acid, at 31 °C. The suspension was sonicated in the same conditions described above for 1 h. After sonication and centrifugation at 100 000g for 1 h at 24 °C in the Beckman R65 rotor, the supernatant containing the unilamellar microvesicles (70% of the initial suspended phospholipid) was then warmed up to 31 °C. An aliquot of 125 mM DOC (in 10 mM Tris, pH 7.5) was rapidly added and mixed to give a final mixture containing a DOC:DMPC ratio of 1:4. The ratio of DOC to DMPC required for macrovesicle formation was determined as described by Enoch & Strittmatter (1979) by measuring the turbidity as a function of the detergent to phospholipid molecular ratio. The turbidity of the solution of DMPC microvesicles increased with increasing amounts of DOC added until a maximal level of turbidity was reached at about 1 mol of DOC per 4 mol of phospholipid. At molecular ratios of DOC to DMPC greater than 0.5, the solutions were essentially clear. The unilamellar macrovesicles began to form immediately, as indicated by the increase in turbidity of the solution at 350 nm. Macrovesicle formation was complete within 10 min at 31 °C. The bulk of the detergent (99.8%) was then removed by passage of the sample (±4 mL) over a Sephadex G-25 (medium porosity) column (60 × 2.5 cm) at 31 °C using the same buffer described above (elution rate, 53 mL/h). Additional chromatography did not remove this residual amount of DOC. The fractions containing the d-UMV were centrifuged at 24 °C for 1 h at 100 000g in the Beckman R65 rotor. The pellet containing the d-UMV (50% of the initial suspended phospholipid) was resuspended in the previously described buffer and kept at room temperature. The final preparation contained 1.8 ± 0.05 DOC molecules per 1000 DMPC molecules. If we assume that the DOC contamination was in the contained volume of d-UMV, the DOC concentration would be around 0.5 mM, or roughly one-tenth the critical micelle concentration of DOC (Helenius & Simons, 1975). The macrovesicles were

<sup>1</sup> Abbreviations used: ANS, 8-anilino-1-naphthalenesulfonate; DMPC, 1- $\alpha$ -dimyristoylphosphatidylcholine; DPPC, 1- $\alpha$ -dipalmitoylphosphatidylcholine; Tris, 2-amino-2-(hydroxymethyl)-1,3-propanediol; EDTA, (ethylenedinitrilo)tetraacetate disodium salt; <sup>31</sup>P NMR, phosphorus-31 nuclear magnetic resonance; NOE, nuclear Overhauser effect; AT, acquisition time; DSC, differential scanning calorimetry; DOC, deoxycholic acid; d-UMV, unilamellar macrovesicles obtained after fusion of microvesicles triggered by deoxycholate (Enoch & Strittmatter, 1979); p-UMV, unilamellar macrovesicles obtained after fusion of microvesicles triggered by the purified *S. pombe* plasma membrane ATPase (Dufour & Tsong, 1981).

stable at this stage for at least 1 week. It must be pointed out that if the same Sephadex G-25 column was used, it had to be extensively washed due to the adsorption of DOC on Sephadex (Carbis et al., 1979). These authors have shown that the partition coefficient ( $K_{av}$ ) for DOC on Sephadex G-25 increases with temperature at low DOC concentrations. Routinely, we washed our column with a volume equivalent to 5 times the total volume of the column. Under these conditions, reproducible preparations were obtained.

The fourth type corresponds to the *ATPase-trigger-fused vesicles* (p-UMV). As reported elsewhere (Dufour & Tsong, 1981), the purified plasma membrane ATPase of the yeast *S. pombe* induces the fusion of DMPC microvesicles below the phase transition of the lipid. A typical procedure was to incubate the purified enzyme with DMPC microvesicles for 2 h at  $9 \pm 1$  °C. The sample was then centrifuged at 100000g in the Beckman R65 rotor for 1 h at 23 °C to form a pellet. The pellet was finally resuspended in the indicated buffer. This suspension was directly used for subsequent analysis. In the samples used, the p-UMV contained 0.005–0.01 mol % of enzyme monomer. Each enzyme monomer contained roughly 70 lipid molecules of a mixed composition (Dufour & Goffeau, 1980b).

**Analytical Procedures.** Protein concentrations were determined by the method of Lowry et al. (1951), using bovine serum albumin as a standard. Phospholipid concentrations were determined by using the modified Bartlett method described by Dittmer & Wells (1969) with the exception that each tube contained 2.4 mL of the following reducing reagent: 1 g of Elon (Kodak) and 3 g of NaHSO<sub>3</sub> per L of double-distilled water. Radioactivity measurements were done by using glass vials contained 20–100  $\mu$ L of sample diluted up to 300  $\mu$ L with distilled water and 3 mL of Liquiscint (National Diagnostics) in a Packard PI TRI-CARB liquid scintillation spectrometer. Lipid phase transitions monitored by turbidity changes at 230 nm, except where otherwise indicated, were taken with a McPherson Model 707K spectrophotometer equipped with an Haake PG 11 temperature programmer. Fusion of DMPC microvesicles induced by the ATPase was followed by monitoring the turbidity changes at 230 nm with the above apparatus. Deoxycholic acid was recrystallized by using the procedure of Soper et al. (1979). Tracer amounts of [*carboxyl*-<sup>14</sup>C]deoxycholic acid were included in detergent solutions to facilitate DOC determinations.

The <sup>31</sup>P NMR spectra were recorded on a Nicolet Technology Corp. TT-23 spectrometer at 40.5 MHz (corresponding to a magnetic field strength of 2.35 T) operating in the Fourier-transform mode. A 2-mm capillary of 0.2 M H<sub>3</sub>PO<sub>4</sub> in 35% HClO<sub>4</sub> was used as a chemical shift reference in some spectra. All NMR experiments were carried out at  $30 \pm 2$  °C unless otherwise stated. The number of scans collected and the cycle time ( $\tau + AT$ ) are indicated under each figure. Filter and sweep widths of 5 and 10 kHz were used for unilamellar and multilamellar vesicles, respectively. For all spectra, an 8K data table was used except where otherwise stated. Phosphorus nuclear spin-lattice relaxation times ( $T_1$ ) were calculated by using a three-parameter-fitting calculation routine (part of the Nicolet Technology Corp. software). For <sup>31</sup>P NMR measurements in the presence of paramagnetic ion, it is necessary to take into account that the inner surface <sup>31</sup>P nuclei will have an NOE enhancement while for the outer surface the NOE will no longer be present due to the electron nuclear dipole-dipole relaxation pathway provided by the paramagnetic metal ion (Yeagle et al., 1975). This potential source of error can be eliminated by properly gating the proton

decoupler so that the NOE is suppressed while the proton decoupling is retained: gated proton decoupling (6-W power level, gated on during acquisition only) was used to eliminate the NOE. For the determination of the outside to inside phospholipid ratio using the paramagnetic ion shift reagent Eu<sup>3+</sup>, enough lanthanide was added to separate the overlapping outside and inside resonances so that their ratio could be accurately measured. The sample volume was 1.5 mL plus 0.25 mL of D<sub>2</sub>O to provide a lock signal. NMR tubes (12 mm) were used, and Teflon vortex plugs were utilized to prevent sample vortexing due to sample spinning.

ANS fluorescence measurements were taken with an Aminco-Bowman spectrofluorometer equipped with a thermostated cell. Excitation and emission wavelengths were 370 and 490 nm, respectively.

Negative staining for electron microscopy analysis was performed as described below, except for p-UMV (see legend of Figure 1). The samples were incubated in 2% ammonium molybdate (pH 7.6) (25  $\mu$ L of sample for every 75  $\mu$ L of stain) at 25 °C for 4–6 h. A 2- $\mu$ L aliquot of the above incubation mixture was applied for 1 min on a glow-discharged (hydrophilic) grid with a carbon-coated parlodion support. The excess sample was drained off and then stained with uranyl formate (0.75%, pH 4.25). Uranyl formate (5  $\mu$ L) was applied to the grid for 15 s. This procedure was repeated twice. The dried grid was finally examined in a Zeiss IO C Transmission Electron Microscope using an accelerating voltage of 60 kV. The sizing of the vesicle preparation was done by measuring the circumference with a HP 9874 A digitizer and a HP 9845 B microcomputer.

Differential scanning microcalorimetry was performed with a MC1 microcalorimeter (Micro Cal, Inc.). Lipid suspension (0.85 mL) ranging from 0.3 to 4 mg/mL concentration was sealed in the calorimeter cell, and a heating rate of 1.5–25 °C/h was employed to obtain the transition curve in heat-capacity form. The heat of transition was determined by planimetry as described by Mabrey & Sturtevant (1979). The van't Hoff enthalpy of a transition was estimated by the relation  $\Delta H_{vH} = 6.9(T_m^2/\Delta T_{1/2})$  where  $\Delta T_{1/2}$  is the width in degrees of the transition curve at the half-height. The cooperative unit, i.e.,  $\Delta H_{vH}/\Delta H_{cal}$  is given only for the purpose of comparison and should not be taken as a unit of the molecular aggregate that undergoes a concerted transition (Kanehisa & Tsong, 1978).

## Results

**Gel Chromatography and Negative Staining.** In the preliminary approach, the several forms of DMPC vesicles were analyzed by gel chromatography and negative-stain electron microscopy, whose advantages and disadvantages have been discussed earlier (Bangham et al., 1974; Szoka & Papahadjopoulos, 1980).

Our DMPC microvesicles were essentially identical with those characterized by Watts et al. (1978). The elution profile for the microvesicles fractionated on Sepharose 4B (Figure 1A) consists only of Huang's peak II, unilamellar vesicles fraction (Huang, 1969). Thus, the sonication and high-speed centrifugation procedure used here produced a lipid dispersion composed of a homogeneous population of unilamellar vesicles with no detectable contamination by multilamellar vesicles. The mean diameter of microvesicles was 260 Å ( $\pm 40$  Å) (Figure 1D). Unchromatographed vesicles were used in our study because, in agreement with previously published data (Marsh et al., 1976; Watts et al., 1978), we have found that chromatographed vesicles were unstable. Figure 1B illustrates the elution pattern of d-UMV on a Sepharose CL-2B column.

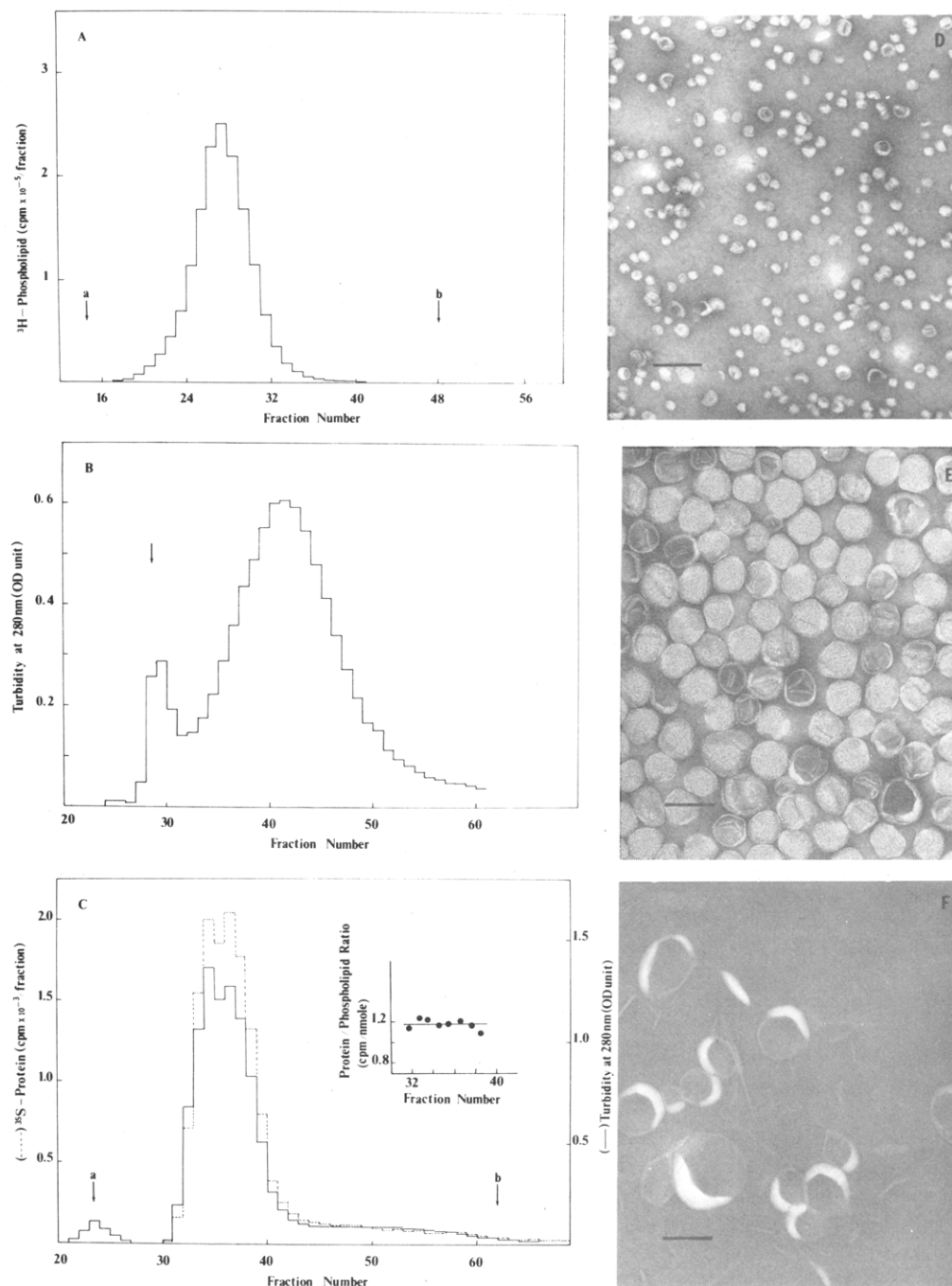


FIGURE 1: Gel chromatography of DMPC microvesicles, d-UMV, and p-UMV. (A) Elution profile of  $^3\text{H}$ -labeled DMPC microvesicles after chromatography on Sepharose 4B. DMPC (40 mg) was dissolved in 1 mL of chloroform and mixed with  $^3\text{H}$ ]DPPC (10 nmol) (13 Ci/mmol). The mixture was evaporated under vacuum to complete dryness and resuspended in 4 mL of 10 mM Tris, 20  $\mu\text{M}$  EDTA, 0.1 M NaCl, and 1 mM  $\text{NaN}_3$  adjusted to pH 7.5 with acetic acid, at 45  $^\circ\text{C}$ . The sample was sonicated at 45  $^\circ\text{C}$  for 1 h (30-min effective sonication time) and centrifuged as described under Materials and Methods. A 800- $\mu\text{L}$  sample of  $^3\text{H}$ -labeled DMPC microvesicles (3.1 mg of phospholipid) was layered on the top of a Sepharose 4B column (53  $\times$  1.7 cm) at 28  $^\circ\text{C}$ , equilibrated with the above buffer. The void volume (Blue dextran) and solvent volume ( $^{14}\text{C}$ ]sucrose) are indicated by arrows a and b, respectively. Fractions of 1.5 mL were collected at an elution rate of 10 mL/h. (B) Turbidity-monitored Sepharose CL-2B elution profile for d-UMV. After Sephadex G-25 chromatography, the d-UMV were pelleted by centrifugation and resuspended in 1.5 mL of buffer as described under Materials and Methods. The d-UMV (27 mg of phospholipid) were layered on the top of a Sepharose CL-2B column (62  $\times$  1.6 cm) and eluted at 30  $^\circ\text{C}$ . Turbidity measurements were done at 280 nm. Other conditions were as described under Materials and Methods. The arrow indicated the void volume. Fractions of 1.5 mL were collected at an elution rate of 10 mL/h. (C) Turbidity and  $^{35}\text{S}$  counts per minute elution profiles for  $^{35}\text{S}$ -ATPase-DMPC fused vesicles. After fusion, the  $^{35}\text{S}$ -ATPase-DMPC fused vesicles were pelleted by centrifugation as described under Materials and Methods. The pellet (13.5 mg of phospholipid, 125  $\mu\text{g}$  of  $^{35}\text{S}$ -labeled protein) resuspended in 650  $\mu\text{L}$  of 10 mM Tris, 20  $\mu\text{M}$  EDTA, 0.1 M NaCl, and 1 mM  $\text{NaN}_3$ , adjusted to pH 7.5 with acetic acid, was layered on top of a Sepharose CL-2B column (53  $\times$  1.6 cm). Elution was done with the above buffer at 15  $^\circ\text{C}$ . Turbidity measurements were at 280 nm. Other conditions were as described under Materials and Methods. The arrows indicated the void volume (a) and DMPC microvesicles peak (b). After phosphate analysis, no phospholipid has been detected in the void volume. Fractions of 1.3 mL were collected at an elution rate of 10 mL/h. The insert gives the  $^{35}\text{S}$  counts per minute per mole of phospholipid through the observed peak. (D) Electron micrograph of negatively stained microvesicles. Conditions were as described under Materials and Methods. The bar represents 100 nm. (E) Electron micrograph of negatively stained d-UMV. An aliquot from the main peak was negatively stained as described under Materials and Methods. The bar represents 100 nm. (F) Electron micrograph of negatively stained p-UMV. Negative staining was performed at 25  $^\circ\text{C}$  with 1% ammonium molybdate solution (pH 6.5). One drop of p-UMV (about 100  $\mu\text{M}$ ) was placed on a formvar-coated grid, and after 5 min, one drop of the staining solution was added; 5 min later, the solution was drained off with filter paper, and the grid was allowed to air-dry and finally examined on a Zeiss 10E electron microscope operated at 60 kV. The bar represents 100 nm.

The main symmetrical, relatively broad peak consists of the so-called d-UMV, characterized by a mean diameter of 900 Å ( $\pm 100$  Å) (Figure 1E). A small peak is also detected in the void volume and consisted of a mixture of both multilamellar and unilamellar vesicles as revealed by DSC analysis, but it consisted of less than 5% of the total phospholipid (data not shown). No contamination by microvesicles was detectable. As will be discussed in the DSC study, use of single fraction and pooled samples gave identical results. Moreover, due to the low yield of the d-UMV in each fraction, NMR study was only done with samples obtained after G-25 column chromatography and high-speed centrifugation. For the p-UMV, the elution pattern on Sepharose CL-2B is given in Figure 1C. One single, symmetrical, and relatively narrow peak, characteristic of a homogeneous population, is obtained. The homogeneity of the p-UMV is also underlined by the constancy of the enzyme to phospholipid ratio by going through the peak as presented in the insert of Figure 1C. Negative-stain electron microscopy analysis of p-UMV reveals single-bilayer pseudospherical vesicles with an average diameter of  $950 \pm 200$  Å (Figure 1F).

**Analyses of the Different DMPC Structures by  $^{31}\text{P}$  NMR.** The  $^{31}\text{P}$  NMR spectrum (Figure 2A) of DMPC microvesicles consists of two peaks having a splitting of 0.1 ppm at 32 °C. The total line width of this "doublet" is  $\sim 9$  Hz (at half-height), in agreement with the 10-Hz value (at 36.4 MHz) reported by de Kruijff et al. (1975). An unexpected observation is that under identical experimental conditions, the inside/outside phosphorus resonances in d-UMV also have resolved chemical shift differences, the  $\delta$  value of this chemical shift (0.22) being approximately twice as large as that observed for the microvesicles. Figure 2B shows this result for d-UMV at 32 °C; the natural line width for the d-UMV preparations is  $\sim 73$  Hz. In contrast, the p-UMV have a single resonance from the inside and outside bilayer head groups and a natural line width of 23 Hz (Figure 2C).  $^{31}\text{P}$  NMR observations of multilamellar vesicles show a spectrum which is significantly broader (Davis, 1972; Sheetz & Chan, 1972), and the line shape is that of the expected powder-type spectrum (Seelig, 1978). Figure 3 shows the spin-lattice relaxation time ( $T_1$ ) measurements for each of the unilamellar vesicle preparations. The  $T_1$ 's for microvesicles, d-UMV, and p-UMV all differ from one another. Data are summarized in Table I which demonstrates that microvesicles and d-UMV are characterized by specific values for chemical shift, line width, NOE, and  $T_1$ . Moreover, comparison of these data supports the contention that the p-UMV are very similar to the d-UMV.

This similarity is further reinforced by the outside to inside phospholipid ratio measurements. It has been shown previously (Bystrov et al., 1971) that  $^{31}\text{P}$  NMR spectroscopy of phospholipid membranes in the presence of paramagnetic ions makes it possible to distinguish between resonances arising from the inner and the outer surfaces of a membrane. In the present study,  $\text{Eu}^{3+}$  was used as the paramagnetic metal ion. It is important to consider that in order for the NMR-paramagnetic metal ion technique to give accurate ratios of the outer to inner phospholipid ratio in a vesicle, several conditions must be met (Hutton et al., 1977), a principal consideration being that the metal ion does not penetrate the bilayer too rapidly. Several successive spectra were monitored after addition of the lanthanide, and the area under the inside peak resonance was plotted against time. As illustrated in Figure 4, the microvesicles are very permeable to the lanthanide with a half-time for the process of 36.5 min. By extrapolating the value for the inside resonance intensity at time zero of the

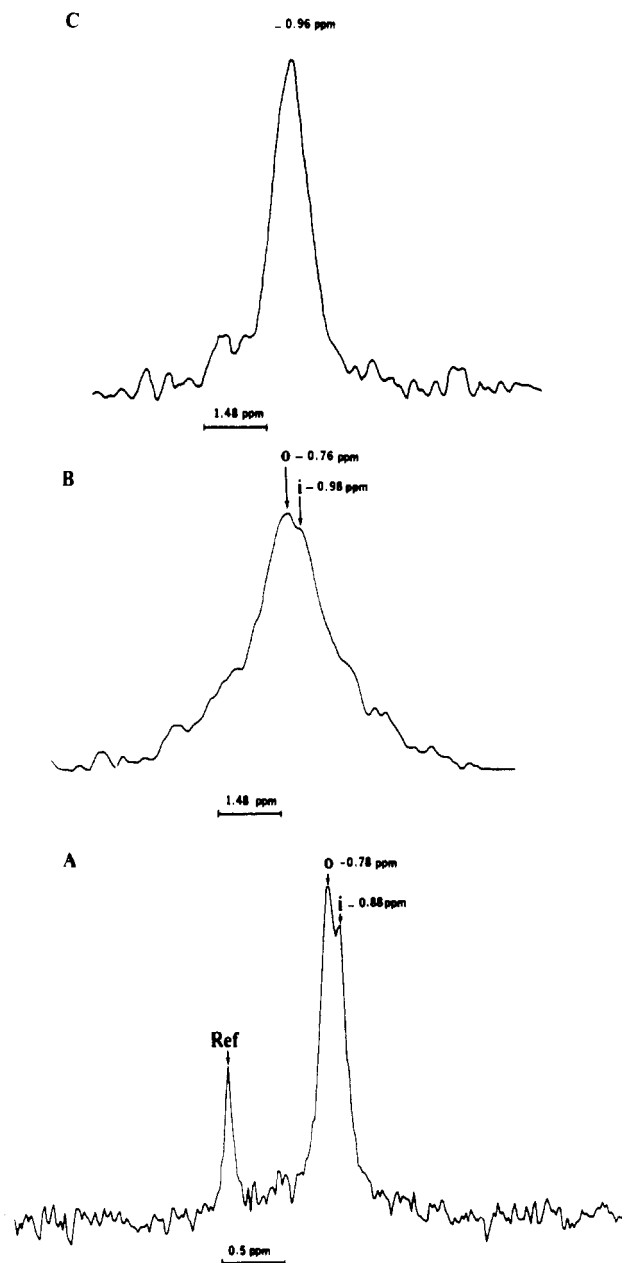


FIGURE 2:  $^{31}\text{P}$  NMR spectra of DMPC microvesicles, d-UMV, and p-UMV. (A)  $^{31}\text{P}$  NMR spectrum of DMPC microvesicles (13 mg of phospholipid/mL) obtained without NOE (128 scans,  $\tau = 2$  s, AT = 1.36 s). For this experiment, a 16K data table was used. The phosphorus standard was also included. The magnetic field scale increases to the right. Other conditions were as described under Materials and Methods. o, outside phospholipid layer; i, inside phospholipid layer. (B)  $^{31}\text{P}$  NMR spectrum of d-UMV (21 mg of phospholipid/mL) obtained without NOE (512 scans,  $\tau = 3$  s, AT = 1.36 s). For this experiment, a 16K data table was used. The magnetic field scale increases to the right. Other conditions were as described under Materials and Methods. o, outside phospholipid layer; i, inside phospholipid layer. (C)  $^{31}\text{P}$  NMR spectrum of p-UMV (7.7 mg of phospholipid/mL, 57  $\mu\text{g}$  of protein) obtained without NOE (512 scans,  $\tau = 2$  s, AT = 1.36 s). For this experiment, a 16K data table was used. The magnetic field scale increases to the right. Other conditions were as described under Material and Methods.

addition of  $\text{EuCl}_3$ , we calculated the outside to inside phospholipid ratio to be 1.94. Multilamellar vesicles are slowly permeable to lanthanide (data not shown) with an outside to inside phospholipid ratio estimated at 0.11. Unlike microvesicles and multilamellar vesicles, no significant lanthanide penetration was observed for d-UMV and p-UMV at least after 4 h (data not shown). Figure 5 shows a typical spectrum for d-UMV and p-UMV; the measured outside to inside

Table I:  $^{31}\text{P}$  NMR Characteristics of Several DMPC Structures at  $30 \pm 2^\circ\text{C}^a$ 

type of structure	chemical shift (ppm)		line width, $\Delta\nu_{1/2}$ (Hz)		NOE (%)	$T_1$ (s)
	proton decoupled	proton coupled	proton decoupled	proton coupled		
unilamellar microvesicles						
outside	-0.78	-0.78				
inside	-0.88	-0.88	9	9	49	$1.41 \pm 0.13$
d-UMV						
outside	-0.76	-0.76				
inside	-0.98	-0.98	73	72	29	$3.79 \pm 0.15$
at $11^\circ\text{C}$		-1.01		471		
multilamellar vesicles	-13.9	-0.67	552	174	100	$0.45 \pm 0.02$
p-UMV						
outside and inside	-0.96	-0.96	23	23	16	$2.71 \pm 0.22$

<sup>a</sup>  $\Delta\nu_{1/2}$  is the width in hertz of the phosphorus resonance measured at half-height. The NOE is the observed change in the intensity of the  $^{31}\text{P}$  signal when the proton spins are saturated (Noggle & Schirmer, 1971). The NOE depends upon a dipole-dipole interaction between the nucleus saturated and the nucleus observed and, in the face of competing interactions, requires these two dipoles be close in space. Removal of the dipoles from close proximity allows competing relaxation mechanisms to become dominant, thereby reducing the NOE.

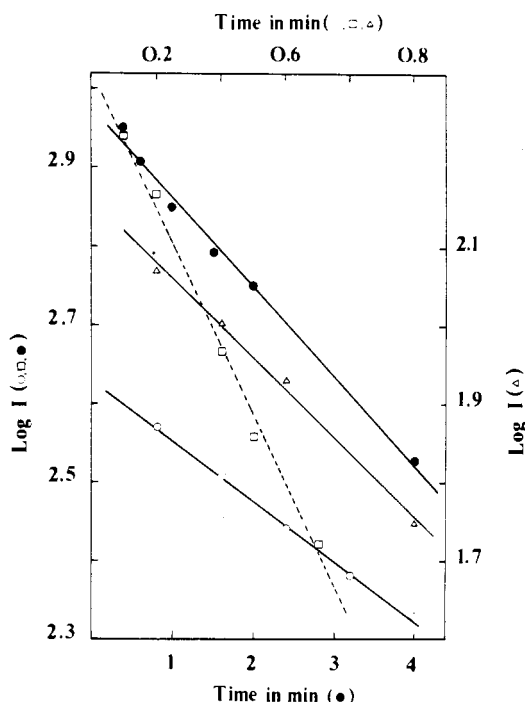


FIGURE 3:  $^{31}\text{P}$  NMR  $T_1$  measurements for the resonances of DMPC microvesicles, d-UMV, multilamellar vesicles, and p-UMV. The medium contained DMPC microvesicles (O) at 13 mg of phospholipid/mL, d-UMV (●) at 21.23 mg of phospholipid/mL, DMPC multilamellar vesicles (□) at 86 mg of phospholipid/mL, or p-UMV (Δ) at 7.65 mg of phospholipid/mL and 57 mg of protein.  $^{31}\text{P}$  NMR spectra were obtained without NOE (for microvesicles, 128 scans,  $\tau = 20$  s, AT = 1.36 s; for d-UMV, 512 scans,  $\tau = 15$  s, AT = 1.36 s; for multilamellar vesicles, 256 scans,  $\tau = 6$  s, AT = 1.36 s; for p-UMV, 256 scans,  $\tau = 20$  s, AT = 0.1 s). Other conditions were as described under Materials and Methods.  $I$  is the normalized integrated intensity of the phosphate group resonance at the corresponding time. For each  $T_1$  measurement, the delay time between subsequent pulses was never less than  $5T_1$ 's in order to get the maximal accuracy for each determination. The  $T_1$  measurements are for both inside and outside resonances.

phospholipid ratios are 1.0 and 1.1, respectively (Table II).

**Analyses of the Different DMPC Structures by ANS Binding.** ANS binding to the outer and inner layers can also be used to determine this outside to inside phospholipid ratio. Indeed, binding and transport studies of ANS across DMPC bilayers have shown that at temperatures below the phase transition of the phospholipid ANS molecules bind only to the outer layer of the vesicles and that transport of ANS across the bilayer occurs near the phase transition temperature, re-

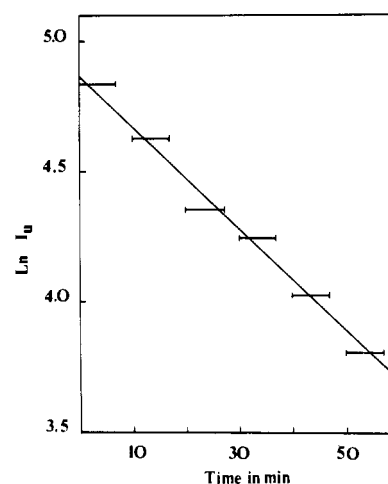


FIGURE 4: Penetration of  $\text{EuCl}_3$  in DMPC microvesicles. DMPC microvesicles (13 mg of phospholipid/mL) and  $^{31}\text{P}$  NMR spectra were obtained by using the conditions described under Materials and Methods. At time zero,  $\text{EuCl}_3$  was added to the sample to  $833 \mu\text{M}$  final concentration. Each point represents an average value of the time required for one spectrum (128 scans,  $\tau = 2$  s, AT = 1.36 s). The time lapse between two successive spectra was 172 s. For each spectrum, the intensity of the unshifted peak ( $I_u$ ) was integrated. The integral of the inside resonance intensity was considered instead of that of the outside resonance intensity. Indeed, the addition of  $\text{EuCl}_3$  shifted and broadened the outside resonance so that part of the outside signal could become lost in the base line, giving rise to a lower outside resonance integral value and subsequently to a wrong outside to inside phospholipid ratio. The initial ratio was calculated by using the following equation:  $[I_i - I_{u(0)}]/I_{u(0)}$  where  $I_i$  and  $I_{u(0)}$  are the intensities before the addition of  $\text{EuCl}_3$  and the extrapolated intensity value at time zero in the presence of  $\text{EuCl}_3$ , respectively.

sulting in binding to the inside layer (Tsong, 1975). In both cases, binding of ANS to the phospholipid layer enhances the fluorescence quantum yield of the dye molecule by 100-fold. The ratio of the outside to inside relative fluorescence intensities of bound ANS can be calculated and used as a marker of the outside to inside phospholipid ratio. From Table II, it appears that both methods give identical results for microvesicles, p-UMV, and d-UMV, confirming that the samples are homogeneous. However, for the multilamellar vesicles, the very low outside fluorescence intensity together with a high scattered light contribution can introduce a large error.

**Differential Scanning Calorimetry Analysis.** A correlation between the activity of membrane-bound or lipid-reconstituted enzymes and motional parameters of the surrounding lipid phase has frequently been sought by comparison of their temperature dependencies (Sandermann, 1978). However, this

Table II: Determination of Outside to Inside Phospholipid Ratio in DMPC Structures<sup>a</sup>

type of DMPC structure	outside/inside phosphorus resonance ratio	outside/inside ANS binding ratio	mean diameter (Å) ± SD
microvesicles	1.9	2.0	260 ± 40
d-UMV	1.0	1.1	900 ± 100
multilamellar vesicles	0.1	<0.1	
p-UMV	1.1	1.1	950 ± 200

<sup>a</sup> For ANS binding, multilamellar vesicles (107 nmol), microvesicles (24 nmol), d-UMV (30 nmol), and p-UMV (368 nmol) were incubated at 13 °C for 20 min in 2 mL of 10 mM Tris, 100 mM NaCl, 1 mM NaN<sub>3</sub>, and 20 μM EDTA adjusted to pH 7.5 with acetic acid, under magnetic stirring and N<sub>2</sub> flux. After this period, 100 μM ANS (10 mM in ethanol) was added. The relative fluorescence intensities observed after 2-s mixing time were taken as the outside ANS binding. The solutions were then incubated at 30 °C for 30 min. After this period, the solutions were put back in the spectrofluorometer at 13 °C in darkness. After a final period of 20 min, the relative fluorescence intensities were measured. These values corresponded to the inside plus outside ANS binding. By difference, the binding to the inside layer was calculated after correction for ANS fluorescence in the absence of the phospholipid and the light scattering signal due to the vesicles. For the outside to inside phosphorus resonance ratio, the values were obtained from the data presented under Figures 6 and 7 or from results not shown.

study usually requires changing the fatty acid and/or polar head group of the phospholipid in order to vary the phospholipid phase transition temperature. The following results show that the same phospholipid can be used if microvesicles and macrovesicles are prepared. Each of the vesicles' preparation has been analyzed by differential scanning calorimetry. The calorimetric transition curves are presented in Figure 6, and the corresponding transition parameters are summarized in Table III. DMPC microvesicles underwent a broad phase transition ( $\Delta T_{1/2} = 7.0$  °C) at 20.3 °C with an associated enthalpy change of 6.73–6.94 kcal/mol. A pretransition not attributable to the multilamellar vesicles or macrovesicles

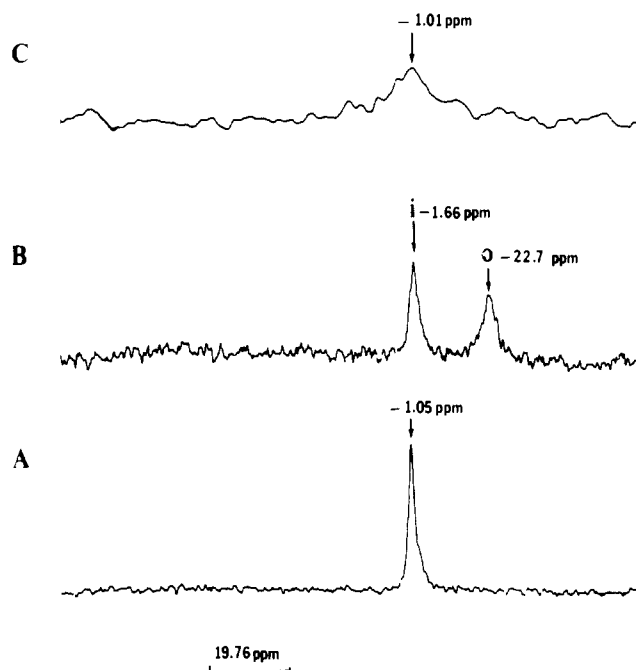


FIGURE 5: <sup>31</sup>P NMR spectra of d-UMV in the presence of lanthanide. <sup>31</sup>P NMR spectra of d-UMV (11.8 mg of phospholipid/mL) were obtained without NOE in the absence (A) (1000 scans,  $\tau = 2$  s, AT = 0.68 s) or in the presence (B) of EuCl<sub>3</sub> (833 μM) (3000 scans,  $\tau = 2$  s, AT = 0.68 s). Spectrum B is plotted at twice the gain of spectrum A. (C) <sup>31</sup>P NMR spectrum of d-UMV (6.89 mg of phospholipid/mL) was obtained without NOE at 11 °C (10887 scans,  $\tau = 0.5$  s, AT = 0.41 s). The magnetic field scale increases to the right. Other conditions were as described under Material and Methods.

contamination was also detected with an optimum at 14.3 °C and an enthalpy change of 0.48–0.63 kcal/mol. Unlike microvesicles, multilamellar vesicles are characterized by a very sharp phase transition at 23.6 °C ( $\Delta T_{1/2} = 0.085$  °C) and a pretransition at 15.5 °C ( $\Delta T_{1/2} = 1.17$  °C). The corresponding enthalpy changes are 5.73 and 0.83 kcal/mol, respectively. The d-UMV DMPC underwent the gel to liquid-

Table III: Transition Properties of Various DMPC Structures<sup>a</sup>

type of DMPC vesicles	footnote	lower transition (pretransition)				upper transition (transition)			
		$T_{m1}$ (°C)	$\Delta T_{1/2}^1$ (°C)	$\Delta H_{1,cal}$ (kcal/mol)	cooperative unit (molecules)	$T_{m2}$ (°C)	$\Delta T_{1/2}^2$ (°C)	$\Delta H_{2,cal}$ (kcal/mol)	cooperative unit (molecules)
microvesicles	e	14.3	2.09	0.48	570	20.3	6.95	6.73	13
	f	14.3	2.09	0.63	430	20.3	6.95	6.94	12
	d					19.0			
d-UMV	b	15	12.3	2.17	22	24.4	0.60	6.8	100
	c	15	12.3	2.17	22	24.4	0.75	6.7	80
	d	12.7				24.0			
	b	15.5	1.17	0.83	590	23.6	0.085	5.73	1300
multilamellar vesicles	b	14.4	1.85	1.06	290	23.6	0.12	5.61	1090
	c	14.1	2.0	1.16	250	23.7	0.19	5.88	560
	d	14.8	1.88	0.31	99	24.4	0.73	5.64	150
p-UMV	b	14.8	1.88	0.31	99	24.4	0.73	5.64	150
	d	12.4				23.8			

<sup>a</sup>  $\Delta T_{1/2}$  is the width in degrees of the excess specific heat vs.  $T$  curve at half-height. The cooperative unit is equal to the ratio of  $\Delta H_{vH}/\Delta H_{cal}$ .  $\Delta H_{vH}$  is the van't Hoff enthalpy calculated by using the following relation:  $\Delta H_{vH} = 6.9(T_m^2/\Delta T_{1/2})$  (Mabrey & Sturtevant, 1979).  $\Delta H_{cal}$  is the calorimetrically determined enthalpy calculated after integration of the calorimetric trace with a planimeter. The cooperative unit is a measure of the cooperativity of the process. The size of the cooperative unit is especially sensitive to impurities and other unrecognized influences (Mabrey & Sturtevant, 1976). <sup>b</sup> Values for first runs. <sup>c</sup> Rerun values of samples after heating up to 95 °C and slowly cooling down. The d-multilamellar vesicles are multilamellar vesicles containing the same residual DOC to phospholipid ratio as that determined for the d-UMV. <sup>d</sup> Turbidity measurements were used for the determination of these values. For DMPC microvesicles, values were calculated by assuming contamination either by macrovesicles (e) or by multilamellar vesicles (f) as described in the legend of Figure 6A.  $T_{m1}$  and  $T_{m2}$  are the temperatures at which the enthalpy changes are half completed.



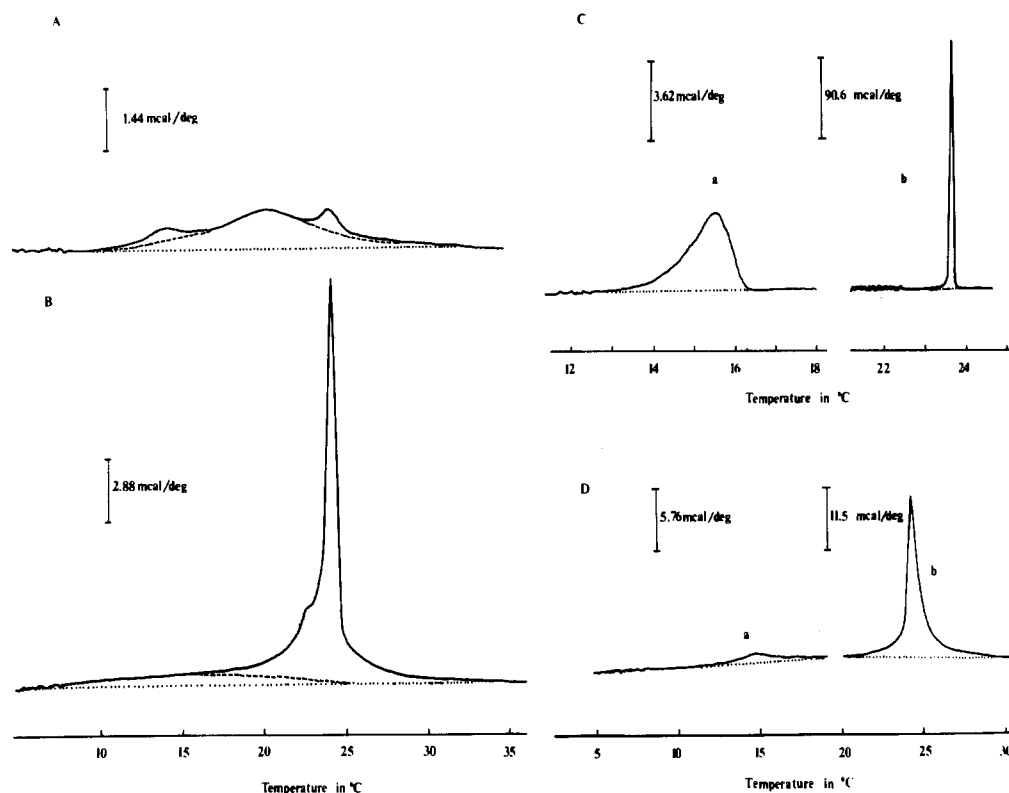


FIGURE 6: Calorimetric transition curves for various DMPC structures. (A) DMPC microvesicles (0.96 mg in 0.85 mL of 10 mM Tris and 20  $\mu$ M EDTA adjusted to pH 7.5 with acetic acid) were scanned at 0.42  $^{\circ}$ C/min. The upper transition parameters were calculated by using the integrated area under the dashed line. The microvesicles concentration was calculated by assuming that the small peak at 24.1  $^{\circ}$ C was due either to macrovesicles or to multilamellar vesicles produced by spontaneous fusion during the incubation at low temperature. With  $\Delta H_{cal}$  equal to 7.2 and 5.73 kcal/mol for the macrovesicles and multilamellar vesicles, respectively, their respective concentrations have been obtained. If we associated the upper peak with multilamellar or macrovesicle contaminations, the enthalpy of this peak corresponds to 13.4% and 10.6% of that expected if all the lipid were in multilamellar or macrovesicular form, respectively. (B) d-UMV (2.55 mg in 0.85 mL of 10 mM Tris, 20  $\mu$ M EDTA, 0.1 M NaCl, and 1 mM  $\text{NaN}_3$  adjusted to pH 7.5 with acetic acid) were scanned at 0.42  $^{\circ}$ C/min. The method used to resolve the calorimetric scan and to calculate the calorimetric parameters is illustrated under the dashed line. (C) Multilamellar vesicles (2.34 mg in 0.85 mL of 10 mM Tris and 20  $\mu$ M EDTA adjusted to pH 7.5 with acetic acid) were scanned at 0.33 (a) and 0.026  $^{\circ}$ C/min (b). (D) p-UMV (4.36 mg of phospholipid in 0.85 mL of 10 mM Tris, 20  $\mu$ M EDTA, 0.1 M NaCl, and 1 mM  $\text{NaN}_3$  adjusted to pH 7.5 with acetic acid) were scanned at 0.42  $^{\circ}$ C/min. The sample contained 55  $\mu$ g of protein. In (a), the ordinate sensitivity was twice as high as that in (b). At the beginning of each curve is given an instrumental tracing.

crystalline phase transition at 24.4  $^{\circ}$ C and had an enthalpy change of 6.8 kcal/mol. Moreover, a shoulder was consistently detected at 22.7  $^{\circ}$ C which was not due to contamination of multilamellar vesicles since addition of multilamellar vesicles left unaltered the peaks at 22.7 and 24.4  $^{\circ}$ C (data not shown). The d-UMV also exhibited a very broad pretransition (Figure 6B) ( $\Delta T_{1/2} = 12.3$   $^{\circ}$ C). Repeated calorimetric scans of d-UMV were superimposable with the initial scans, indicating that the vesicles were stable for the time course of the experiments (data not shown). Moreover, scanning of the d-UMV after heating up to 95  $^{\circ}$ C introduced little change in the transition parameters (Table III). This is in contrast to the small sonicated DMPC vesicles and the multilamellar vesicles; the former were transformed to a mixture of different vesicle forms (data not shown), and the transition width of the latter was very much broadened. The presence of 0.16 mol % of DOC in the multilamellar vesicles did not change the transition temperatures of this vesicle form. Nor did this amount of DOC contamination broaden the transition width to the extent observed for d-UMV and p-UMV systems (Table III). DSC analysis of fractions obtained after Sepharose CL-2B column chromatography, presented in Figure 7, showed that all calorimetric characteristics including  $T_m$ ,  $\Delta H_{cal}$ , and  $\Delta T_{1/2}$  were identical with or similar to the pooled sample, suggesting that size distribution is not a source of the broadness of the transition. The ATPase-Trigger-fused vesicles showed pretransition and transition phases at 14.8 and 24.4  $^{\circ}$ C, respec-

tively. The enthalpy changes associated with the pretransition and transition steps are 0.31 and 5.64 kcal/mol. Finally, it must be mentioned that both pretransition and transition of p-UMV, d-UMV, and multilamellar vesicles are clearly detectably by monitoring the turbidity changes of the suspension by increasing temperature [Figure 8 and Tsong & Kanehisa (1977)].

## Discussion

**Negative-Stain Electron Microscopy and Gel Chromatography.** Negative-stain electron microscopy indicates that the final fused vesicles triggered by the plasma membrane ATPase have the same average diameter as those fused in the presence of DOC, 950 and 900  $\text{\AA}$ , respectively. This suggests that a mean diameter of 1000  $\text{\AA}$  could be a limiting value for DMPC macrovesicles which are highly stable thermodynamically. These macrovesicles correspond to a 3.5- and 45-fold increase in diameter and total volume, respectively, compared to those values for the original microvesicles. Multilamellar material was not seen in any of the samples although the resolution was probably not adequate to distinguish between vesicles with one or two lamellae. Generally, the interiors of the vesicles are not stained, so the number of lamellae could not be assessed with confidence, this being presumably because the bilayers are impermeable to the stain. However, it is important to note that no multilamellar vesicles were detected after gel chromatography of either microvesicles of p-UMV. Only in the



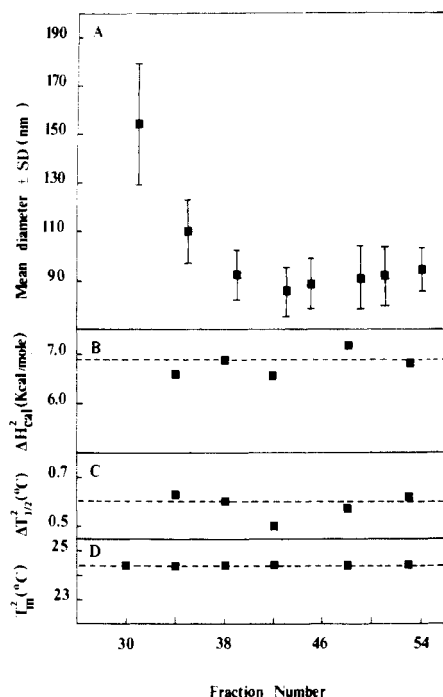


FIGURE 7: Size distribution and calorimetric parameters of fractions after gel chromatography on Sepharose CL-2B. Conditions were as described in the legend of Figure 1B. (A) Size distribution: negative staining and vesicle sizing were as described under Materials and Methods.  $\Delta H_{cal}^2$  (B),  $\Delta T_{1/2}^2$  (C), and  $T_m^2$  (D) were calculated for samples from each fraction (scanning rate of 0.42 °C/min). Other conditions were as described under Materials and Methods. Dashed lines represent values of the pooled sample.

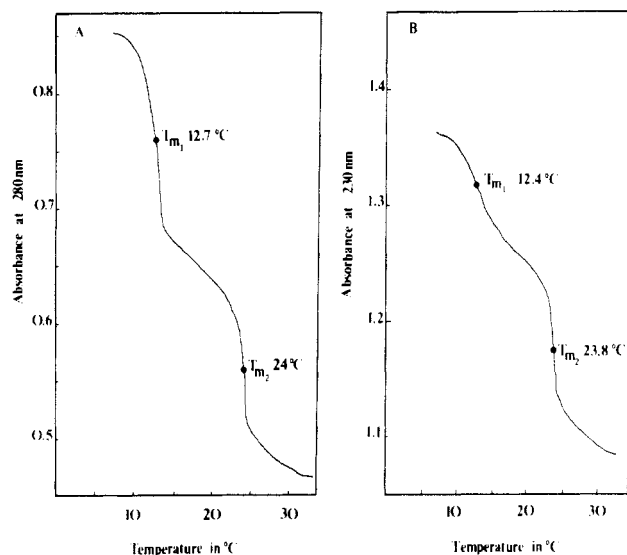


FIGURE 8: Equilibrium transition curves of d-UMV and p-UMV. Only the heating curves are shown. (A) d-UMV (1.37 mg of phospholipid in 1 mL of 10 mM Tris, 20  $\mu$ M EDTA, 0.1 M NaCl, and 1 mM Na<sub>3</sub>N<sub>3</sub> adjusted to pH 7.5 with acetic acid) were scanning at 18 °C/h. Turbidity changes at 280 nm were monitored. The measurement was started after a period of 5 h at 5 °C. (B) p-UMV (0.9 mg of phospholipid and 11  $\mu$ g of protein in 1.3 mL of 10 mM Tris, 20  $\mu$ M EDTA, 0.1 M NaCl, and 1 mM Na<sub>3</sub>N<sub>3</sub> adjusted to pH 7.5 with acetic acid) were scanned at 18 °C/h. Turbidity changes at 230 nm were monitored. The measurement was started after overnight incubation in the refrigerator. Other conditions were as described under Materials and Methods.

case of the d-UMV with a slight contamination (<5%) by large materials been observed.

**<sup>31</sup>P NMR Studies.** The outside to inside phospholipid ratio, which reflects vesicle size, number of bilayers in the vesicles, and leakiness of the vesicles to lanthanide, can accurately be

determined by NMR paramagnetic ion shift reagent studies (Hutton et al., 1977; Bergelson, 1978). Since no significant aggregation or fusion of the microvesicles occurs in presence of Eu<sup>3+</sup>, it is obvious from the data of Figure 4 that paramagnetic ions penetrate into the internal cavity of the DMPC microvesicles, in agreement with previous workers (Hauser & Barrat, 1973) who have observed that short-chain lecithins are not effective cation barriers. This contrasts with what is generally observed with egg phosphatidylcholine or DPPC (Bystrov et al., 1971; Berden et al., 1975; Hauser et al., 1972; de Kruijff et al., 1975; Levine et al., 1973). Of some importance is the fact that inner and outer signals in the <sup>31</sup>P NMR spectra of d-UMV and p-UMV recorded in the presence of externally added EuCl<sub>3</sub> are not changed during incubation for many hours (at least 4 h). This implies that the vesicles are not permeable to Eu<sup>3+</sup> ions. Moreover, it may be concluded that the ATPase or residual DOC does not disturb the integrity of the bilayer. The extrapolated 1.94 ratio of microvesicles is in good agreement with previously reported values for other vesicle compositions (Hutton et al., 1977; Bergelson, 1978). A value of 2.65 was reported by de Kruijff et al. (1975). The permeability of DMPC microvesicles which was not considered in that work is presumably the source of this discrepancy. The ratio close to 1 for d-UMV and p-UMV argues for a similar packing of both outside and inside phospholipid layers. Schwartz & McConnell (1978) using the spin-label reduction method have observed that DMPC multilamellar vesicles dispersed by vigorous vortexing have an average value of 9% of external lipid which is very similar to the 9.9% reported here (Table II). Our data on the microvesicles, p-UMV, and d-UMV are in agreement for expected line shape and line width when compared to the result of Burnell et al. (1980).

**DSC Analysis.** Multilamellar aqueous suspensions of DMPC are characterized by a highly cooperative phase transition (cooperative unit = 1300;  $\Delta T_{1/2}$  = 0.085 °C) at 23.6 °C and an additional broader transition of lower enthalpy occurring at 15.5 °C [Table III; for a review, see Mabrey & Sturtevant (1979)]. This high value of the cooperative unit we obtained leads us to conclude that the commercial DMPC used in this work is very pure. Indeed, in their study of the gel to liquid-crystalline phase transition of a several times crystallized sample of DPPC, Albon & Sturtevant (1978) obtained a  $\Delta T_{1/2}$  of 0.067 °C and concluded that the crystalline sample had a purity of at least 99.94 mol %. Unlike multilamellar vesicles, DSC studies of unilamellar vesicles have received little attention. As shown in Figure 6, the microvesicles, whose stability depends more on experimental conditions, present a complex DSC spectrum, with three clearly separable peaks. A small, sharper peak at 24.1 °C was treated as resulting from fused vesicles and was estimated to constitute about 10% of total lipid mass (see legend in Figure 6). The broad peak around 14 °C was consistently observed, and it cannot be accounted for by assuming that it is the pretransition of the 10% contamination of fused vesicles. The half-width of this transition was difficult to estimate because it was overshadowed by the main transition at 20.3 °C. The higher enthalpy (6.7–6.9 kcal/mol) associated with the main transition of DMPC microvesicles disagrees with previously reported values of 0.9 (Kantor et al., 1977), 3.3 (Melchior & Stein, 1976), and 4.3 kcal/mol (Mabrey, in Eisenberg & Crothers, 1979). This large discrepancy may be due to the difficulty in assigning the base line because of the very broad transition curve. However, by using higher concentrations (1.5–9 mg/mL) of lipid and repeated experiments, we are

confident that the value we report here cannot be off more than 10%. In fact, the data given in Table III show that unilamellar vesicle systems generally have a higher enthalpy change for the gel to liquid-crystalline phase transition than that of the multilamellar vesicles.

Another interesting observation in the DSC experiment is that both the d-UMV and the p-UMV exhibited much broader gel to liquid-crystalline phase transitions as compared to that of the multilamellar vesicles. The transition temperatures of the former are also consistently higher (0.7 °C) than that of the latter. As mentioned, the broadening of the d-UMV transition cannot be attributed to the DOC contamination since the addition of the same amount of DOC (0.2 mol %) to multilamellar vesicles resulted in only a slight broadening of  $\Delta T_{1/2}$  (from 0.085 to 0.12 °C). The broadening can also not be attributed to the size distribution of the macrovesicles, since samples taken from the peak area of the Sepharose CL-2B elution profile (Figure 1B) gave identical transition curves (Figure 7). The d-UMV are extremely stable. A sample heating up to 95 °C followed by a slow overnight cooling gave an unaltered thermal transition curve. This is not the case for other vesicle systems, i.e., the unilamellar microvesicles and multilamellar vesicles. The above result suggests that the unilamellar macrovesicles may be a thermodynamically stable form of DMPC assemblies in water and also that in the multilamellar system interlayer interactions may contribute strongly to the cooperativity of the phase transition. Finally, a comparative study of the d-UMV, p-UMV, and multilamellar vesicles points out a high analogy between these structures. In a recent study using octyl glucoside to produce DPPC large vesicles (600–2100 Å in diameter), Petri et al. (1980) have also shown that the vesicles so obtained have thermal characteristics similar to those of multilamellar suspensions. However, the high-sensitivity calorimeter we employed here allows us to see some subtle differences which may prove to be important for elucidating interlayer interactions in liposome system.

In conclusion, it appears that all listed characteristics are interrelated, and together they form a solid base for comparison of various vesicles. The negative-stain electron microscopy, molecular sieve chromatography,  $^{31}\text{P}$  NMR, and DSC results all strongly indicate that large structures of DMPC triggered by the purified plasma membrane ATPase of yeast at temperatures below the gel to liquid-crystalline phase transition are macrovesicles. All data lead to the conclusion that ATPase-DMPC-fused vesicles are stable unilamellar vesicles about 950 Å in diameter. These large vesicles present intact barriers to ion permeation at 30 °C, the optimum temperature of plasma membrane ATPase activity. These ATPase-fused vesicles provide, thus, an attractive model for investigating the assumed proton-pumping activity of this enzyme (Foury & Goffeau, 1975; Foury et al., 1977; Serrano, 1980). Indeed, we have observed that these ATPase-fused vesicles are characterized by a very low ATPase activity not attributable to enzyme denaturation or an orientation problem (Dufour & Tsong, 1981), which might indicate a high coupling between ATP hydrolysis and  $\text{H}^+$  pumping. Work is currently being carried out to answer this important question.

#### Acknowledgments

We are grateful to Dr. U. Aepli for the use of his electron microscope.

#### References

Albon, N., & Sturtevant, J. M. (1978) *Proc. Natl. Acad. Sci. U.S.A.* 75, 2258–2260.

- Amory, A., Foury, F., & Goffeau, A. (1980) *J. Biol. Chem.* 255, 9353–9357.
- Bangham, A. D., Hill, M. W., & Miller, N. G. (1974) *Methods Membr. Biol.* 1, 1–68.
- Berden, J. A., Barker, R. W., & Radda, G. K. (1975) *Biochim. Biophys. Acta* 375, 186–208.
- Bergelson, L. D. (1978) *Methods Membr. Biol.* 9, 275–335.
- Burnell, E. E., Cullis, P. R., & de Kruijff, B. (1980) *Biochim. Biophys. Acta* 603, 63–69.
- Bystrov, V. F., Dubrovina, N. I., Barsukov, L. I., & Bergelson, L. D. (1971) *Chem. Phys. Lipids* 6, 343–350.
- Carbis, R. A., Rodda, S. J., & Hampson, A. W. (1979) *J. Chromatogr.* 173, 182–186.
- Davis, D. G. (1972) *Biochem. Biophys. Res. Commun.* 49, 1492–1497.
- de Kruijff, B., Cullis, P. R., & Radda, G. K. (1975) *Biochim. Biophys. Acta* 406, 6–20.
- Dittmer, J. C., & Wells, M. A. (1969) *Methods Enzymol.* 14, 483–530.
- Dufour, J.-P., & Goffeau, A. (1978) *J. Biol. Chem.* 253, 7026–7032.
- Dufour, J.-P., & Goffeau, A. (1980a) *Eur. J. Biochem.* 105, 145–154.
- Dufour, J.-P., & Goffeau, A. (1980b) *J. Biol. Chem.* 255, 10591–10598.
- Dufour, J.-P., & Tsong, T. Y. (1981) *J. Biol. Chem.* 256, 1801–1808.
- Dufour, J.-P., Boutry, M., & Goffeau, A. (1980) *J. Biol. Chem.* 255, 5735–5741.
- Eisenberg, D., & Crothers, D. (1979) *Physical Chemistry with Applications to the Life Sciences*, Benjamin/Cummings, New York.
- Enoch, H. G., & Strittmatter, P. (1979) *Proc. Natl. Acad. Sci. U.S.A.* 76, 145–149.
- Foury, F., & Goffeau, A. (1975) *J. Biol. Chem.* 250, 2354–2362.
- Foury, F., Boutry, M., & Goffeau, A. (1977) *J. Biol. Chem.* 252, 4577–4583.
- Hauser, H., & Barrat, M. D. (1973) *Biochem. Biophys. Res. Commun.* 53, 399–405.
- Hauser, H., Phillips, M. C., & Stubbs, M. (1972) *Nature (London)* 239, 342–344.
- Helenius, A., & Simons, R. (1975) *Biochim. Biophys. Acta* 415, 29–79.
- Huang, C. (1969) *Biochemistry* 8, 344–351.
- Hutton, W. C., Yeagle, P. L., & Martin, R. B. (1977) *Chem. Phys. Lipids* 19, 255–265.
- Kanehisa, M. I., & Tsong, T. Y. (1978) *J. Am. Chem. Soc.* 100, 242–432.
- Kantor, K. L., Mabrey, S., Pretegard, J. H., & Sturtevant, J. M. (1977) *Biochim. Biophys. Acta* 466, 402–410.
- Levine, Y. K., Lee, A. G., Birdsall, N. J., Metcalfe, J. C., & Robinson, J. D. (1973) *Biochim. Biophys. Acta* 291, 592–607.
- Lowry, O. H., Rosebrough, N. J., Farr, A. L., & Randall, R. J. (1951) *J. Biol. Chem.* 193, 265–275.
- Mabrey, S., & Sturtevant, J. M. (1976) *Proc. Natl. Acad. Sci. U.S.A.* 73, 3862–3866.
- Mabrey, S., & Sturtevant, J. M. (1979) *Methods Membr. Biol.* 9, 237–274.
- Marsh, D., Watts, A., & Knowles, P. F. (1976) *Biochemistry* 15, 3570–3578.
- Melchior, D. L., & Steim, J. M. (1976) *Annu. Rev. Biophys. Bioeng.* 5, 205–238.

- Noggle, J. H., & Schirmer, R. E. (1971) *The Nuclear Overhauser Effect*, Academic Press, New York.
- O'Neill, I. K., & Richards, C. P. (1980) *Annu. Rep. NMR Spectros.* 10A, 133-236.
- Petri, W. A., Jr., Estep, T. N., Pal, R., Thompson, T. E., Biltonen, R. L., & Wagner, R. R. (1980) *Biochemistry* 19, 3088-3091.
- Sandermann, H., Jr. (1978) *Biochim. Biophys. Acta* 515, 209-237.
- Schwartz, M. A., & McConnell, H. M. (1978) *Biochemistry* 17, 837-840.
- Seelig, J. (1978) *Biochim. Biophys. Acta* 515, 105-140.
- Serrano, R. (1980) *Eur. J. Biochem.* 105, 419-442.
- Sheetz, M., & Chan, S. (1972) *Biochemistry* 11, 4573-4581.
- Soper, J. W., Decker, G. L., & Pedersen, P. L. (1979) *J. Biol. Chem.* 254, 11170-11176.
- Szoka, F., Jr., & Papahadjopoulos, D. (1980) *Annu. Rev. Biophys. Bioeng.* 9, 467-508.
- Tsong, T. Y. (1975) *Biochemistry* 14, 5409-5414.
- Tsong, T. Y., & Kanehisa, M. I. (1977) *Biochemistry* 16, 2674-2680.
- Watts, A., Marsh, D., & Knowles, P. F. (1978) *Biochemistry* 17, 1792-1801.
- Yeagle, P. L., Hutton, W. C., Huang, C., & Martin, R. B. (1975) *Proc. Natl. Acad. Sci. U.S.A.* 72, 3477-3481.

## Partial Characterization of Sialoglycopeptides Produced by Cultured Human Melanoma Cells and Melanocytes†

V. P. Bhavanandan,\* Anne W. Katlic, John Banks, Jeffrey G. Kemper, and Eugene A. Davidson

**ABSTRACT:** The sialoglycopeptides produced by HM7 human melanoma and fetal uveal melanocyte cultures grown in the presence of [<sup>3</sup>H]glucosamine and [<sup>35</sup>S]sulfate were isolated from the Pronase digests of cells, spent media, and intracellular material. From the melanoma culture, six sialoglycopeptides, accounting for 43% of the total <sup>3</sup>H radioactivity in the non-diffusible cell-associated glycopeptides, were purified. A major glycopeptide (GPIb) having an apparent molecular weight in the range 12 000-15 000 showed specific sialic acid dependent interaction with wheat germ agglutinin (WGA). It was found to contain mainly O-glycosidically linked oligosaccharides having the structure (AcNeu)→<sub>0-2</sub>[Gal→GalNAc]; some N-glycosidically linked saccharides were also present. A

second WGA-binding glycopeptide (GPIa) was smaller and less anionic and had a higher proportion of N-glycosidically linked saccharides than GPIb. The normal fetal cultures yielded either no (iris) or markedly reduced (melanocytes) quantities of the WGA-binding glycopeptides. The four WGA-nonbinding sialoglycopeptides purified from melanoma were shown to have complex (N-acetylactosaminyl type) oligosaccharides linked via N-acetylglucosamine to asparagine with either no or insignificant amounts of O-glycosidically linked saccharides. The corresponding glycopeptides from melanocytes were of smaller molecular size and lower anionic charge, reflecting an overall lower degree of glycosylation.

Differences in the glycoproteins produced by malignant cells compared to normal cells have been reported (Bramwell & Harris, 1978; Buck et al., 1979; Ceccarini & Atkinson, 1977; Codington et al., 1979; Glick, 1979; Muramatsu et al., 1979; Takasaki et al., 1980; van Beek et al., 1977). A molecular description of these alterations is of importance because it will help to understand the biological properties of malignant cells.

We have investigated in some detail the glycoproteins and glycopeptides isolated from B16 mouse melanoma cells grown in culture and in vivo. The characterization of a mucin-type sialoglycopeptide (Bhavanandan & Davidson, 1976; Bhavanandan et al., 1977; Fareed et al., 1978) and a melanoma-associated antigen (Bhavanandan et al., 1980) have been reported. The characterization of a malignancy-related mucin-type sialoglycopeptide produced by human breast cancer cell lines has also been reported (Chandrasekaran & Davidson, 1979).

We report here the purification and partial structures of the major glycopeptides isolated from cultured human melanoma cells and from the culture media. These are compared to those

produced by normal fetal melanocytes in culture. The glycopeptides obtained from the highly tumorigenic (in athymic mice) human melanoma cells are markedly different from those obtained from nontumorigenic human fetal uveal melanocytes. A preliminary report of these results has been presented (Bhavanandan et al., 1979).

### Experimental Procedures

**Materials.** The cells and culture conditions used are described in the following paper in this issue (Bhavanandan, 1981). Neuraminidase (*Vibrio cholerae*) was from Calbiochem. Bio-Gel P-2, P-4, P-6, and P-10 were obtained from Bio-Rad Laboratories (Richmond, CA). DEAE-Sephacel, DEAE-Sephacel CL-6B, Sephadex G-50, and Sephacryl S-200 were purchased from Pharmacia (Piscataway, NJ).  $\beta$ -Galactosidase,  $\beta$ -N-acetylhexosaminidase, and endo- $\alpha$ -N-acetylglucosaminidase from *Diplococcus pneumoniae* culture filtrates were prepared in this laboratory. These enzymes were free of contaminating glycosidases as tested with *p*-nitrophenyl glycosides and isotopically labeled natural substrates (fetuin or pig submaxillary mucin glycopeptides) (Umemoto et al., 1977). Endo- $\beta$ -N-acetylglucosaminidase D (Muramatsu et al., 1978) and endo- $\beta$ -N-acetylglucosaminidase H (Tarentino & Maley, 1974) were purchased from Miles (Elkhart, IN). Highly purified exo- $\beta$ -galactosidase from jack bean (Li et al., 1975) and endo- $\beta$ -galactosidase from *Escherichia freundii*

† From the Department of Biological Chemistry and The Specialized Cancer Research Center, The Milton S. Eshelman Medical Center, The Pennsylvania State University, Hershey, Pennsylvania 17033. Received November 10, 1980. This research was supported by Research Grants CA15483 and CA17686 from the U.S. Public Health Service.